Int. J. Bio-Inorg. Hybr. Nanomater., 7(3): 255-265, Autumn 2018

Investigation of Sup90-Dota and interaction with Carbon nanotubes; A Semi-empirical study

R. Mohammadi[1], R. Rasoolzadeh[2], A. Esfarjani[3]*

[1,2,3] *Faculty of Science, Najafabad Branch, Islamic Azad University, Najafabad, Isfahan, Iran*

Received: 30 May 2018; Accepted: 4 August 2018

ABSTRACT: The investigation of the anticancer drugs will be important because of the proliferation of cancer. We want to take steps to improve public health. The combination of two carbon nanotubes (single wall nanotube and multi-wall nanotube) and Sup90-Dota (an anticancer drug) was investigated based on Molecular Mechanic and Semi-Empirical methods. Our goal is to investigate the transfer of carbon nanotubes by drug Sup90- Dota and the study of structural changes caused by the interaction of this anticancer drug combination with the nanotubes. We study of different parameters such as total energy, potential energy and kinetic energy and time of simulations are 20 ns. Calculation and geometrical optimization in different temperature (295,298,310 and 315 Kelvin) were conducted via Monte Carlo method (Amber, Bio^+, MM^+, and OPLS). The semi-empirical calculations such as total energy, binding energy, isolated atomic energy, electronic energy, core–core interaction and heat of formation in AM1, RM1, PM3, MNDO, INDO and CNDO for Sup90- Dota and CNT- Sup90- Dota complex. Analysis of Sup90- Dota and its interaction with CNTs show that this carrier can be applied to improve the activities of this anti-cancer drug.

Keywords: *Anticancer; Carbon Nanotube; Molecular Mechanic; Semi-Empirical; Sup90 – Dota.*

INTRODUCTION

Hepatocellular carcinoma (HCC) is the most common type of primary liver cancer in adults and is the most common cause of death in people with cirrhosis (Forner, *et al.*, 2012). It occurs in the setting of chronic liver inflammation and is most closely linked to chronic viral hepatitis infection (hepatitis B or C) or exposure to toxins such as alcohol or aflatoxin. Certain diseases, such as hemochromatosis and alpha 1-antitrypsin deficiency, markedly increase the risk of developing HCC. Metabolic syndrome and NASH are also increasingly recognized as risk factors for HCC (Kumar, *et al.*, 2015). As with any cancer, the treatment and prognosis of HCC vary depending on the specifics of tumor histology, size, how far cancer has spread, and overall health. The vast majority of HCC occurs in Asia and sub-Saharan Africa, in countries where hepatitis B infection is endemic and many are infected from birth. The incidence of HCC in the United States and other developing

(*) Corresponding Author - e-mail: Reza.Rasoolzadeh@yahoo.com

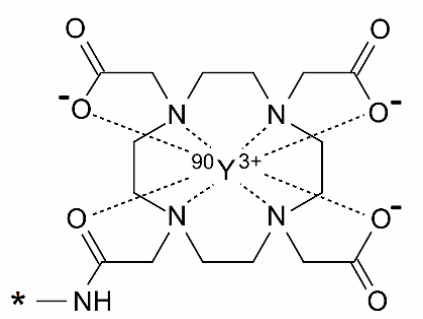

Scheme 1. Yttrium-90Y tacatuzumab tetraxetan structure

countries is increasing due to an increase in hepatitis C virus infections. It is more common in male than females for unknown reasons (Kumar, *et al.*, 2015). Yttrium-90, 90Y, is a medically significant isotope of yttrium (Scheme 1) (DeVita, *et al.*, 2008).

Yttrium-90 has a wide and valuable use in radiation therapy to treat cancer (Kheyfits, 2010). Yttrium isotopes are among the most common products of the nuclear fission of uranium in nuclear explosions and nuclear reactors. In the context of nuclear waste management, the most important isotopes of yttrium are 91Y and 90Y, with half-lives of 58.51 days and 64.1 hours, respectively (Sonzogni, 2008). Though 90Y has a short half-life, it exists in secular equilibrium with its long-lived parent isotope, strontium-90 (90Sr) with a half-life of 29 years (Lide, 2007-2008). Yttrium isotopes with mass numbers at or below 88 decay primarily by positron emission (proton → neutron) to form strontium (Z = 38) isotopes (Sonzogni, 2008). Yttrium isotopes with mass numbers at or above 90 decay primarily by electron emission (neutron → proton) to form zirconium (Z = 40) isotopes (Sonzogni, 2008). Isotopes with mass numbers at or above 97 are also known to have minor decay paths of β− delayed neutron emission (Audi, *et al.*, 2003). 90Y undergoes β− decay to zirconium-90 with a half-life of 64.1 hours (Y-90 Handling Precautions, 2015) and decay energy of 2.28 MeV (Chu, *et al.*, 1999). It also produces 0.01% 1.7 MeV (Rault, *et al.*, 2009) photons along the way. Interaction of the emitted electrons with matter can lead to Bremsstrahlung radiation. Yttrium-90 is a decay product of strontium-90 which makes up about 5% of the nuclear daughter isotopes when uranium is fission (Strontium, Radiation Protection, US EPA. EPA. 2012). Yttrium-90 is produced by chemical high-purity separation from strontium-90, a fission product of uranium in nuclear reactors (PNNL: Isotope Sciences Program-Yttrium-90 Production. PNNL. 2012). 90Y plays a significant role in the treatment of hepatocellular carcinoma (HCC) and other liver cancers. Trans-arterial radioembolization is a procedure performed by interventional radiologists in which microspheres are impregnated with 90Y and injected into the arteries supplying the tumor (Kallini, *et al.*, 2016). Radioembolization with 90Y significantly increases time-to-progression (TTP) of HCC, (Salem, *et al.*, 2016) has a tolerable adverse event profile and improves patient quality of life more than do similar therapies (Salem, *et al.*, 2013).

COMPUTATIONAL METHODS

Many studies have shown that the carbon nanotubes pos- sess remarkable mechanical and physical properties lead- ing too many potential applications such as fluid trans- port, fluid storage at the nanoscale, and Nano devices for drug delivery (Moghaddam, *et al.*, 2016). We used the methods Molecular Dynamics, Monte Carlo and the force fields are AMBER, BIO, MM+ and OPLS and temperatures are 292, 298, 310, and 315 (Besharati & Rasoolzadeh, 2014). The molecular mechanics method using the MM+ force field, and the Austin Model 1 (AM1) and Parameterized Model number 3 (PM3) semi-empirical method within the Restricted Hartree–Fock (RHF) formalism are sufficient to study carbon systems. In 1989, Stewart improved the techniques of parameterization and published PM3, which gave lower average errors than AM1, are suffi- cient to study carbon systems, mainly for the enthalpies of formation (Moghaddam, *et al.*, 2016). In the first step of the calculations we optimized the geometry and defined Potential Energy of the nanotube structure by performing molecular mechanics calcula- tion using MM+ and other force fields, if too large a time step is used in Monte Carlo simulation, it is possible to have a basic instability in the equations that result in a mol- ecule blowing apart. In the next step, we calculated the Vibrational modes of the tube by applying the semi-empirical molecular orbital method by the Hyperchem-8.0 package

Table 1. Amber force field of sup-90

T(K)	Time step Ns	mw-sup90-DOTA-Hmn14(Kcal/mol)			sw-sup90-DOTA-Hmn14(Kcal/mol)			sup90-DOTA-Hmn14(Kcal/mol)		
		Kinetic energy	Potential energy	Total energy	Kinetic energy	Potential energy	Total energy	Kinetic energy	Potential energy	Total energy
315	10	319.2423	11053.95	11373.2	153.9875	1221.903	1375.891	50.7032	93.99608	144.6993
	20		6498.869	6818.111		1029.169	1183.157		91.3849	142.0881
	30		4945.695	5264.937		867.3067	1021.294		90.10798	140.8112
	40		4152.365	4471.607		742.6955	896.683		90.17609	140.8793
	50		3557.814	3877.056		698.2619	852.2494		100.8746	151.5778
	60		3046.39	3365.632		677.0221	831.0096		105.719	156.4222
	70		2794.597	3113.839		657.8353	811.8227		97.3307	148.0339
	80		2605.588	2924.831		633.3303	787.3178		98.54313	149.2463
	90		2464.788	2784.031		629.3676	783.3551		94.05946	144.7627
	100		2367.383	2686.625		632.6485	786.636		94.5214	145.2246
310	10	314.175	11313.57	11627.75	151.5432	1219.897	1371.44	49.89838	92.23149	142.1299
	20		6648.351	6962.526		1020.285	1171.829		89.57556	139.4739
	30		4983.792	5297.967		842.0329	993.5761		93.68669	143.5851
	40		4153.527	4467.702		745.3585	896.9017		90.92374	140.8221
	50		3599.669	3913.844		694.3882	845.9314		97.00292	146.9013
	60		3205.394	3519.569		665.7893	817.3325		99.80938	149.7078
	70		2883.74	3197.915		661.9889	813.5321		89.04395	138.9423
	80		2664.312	2978.487		654.17	805.7133		97.34331	147.2417
	90		2519.026	2833.201		636.0014	787.5446		101.2334	151.1318
	100		2373.161	2687.336		621.5661	773.1093		101.3584	151.2568
298	10	302.0134	11212.08	11514.1	145.677	1201.63	1347.307	47.96683	161.3123	209.2791
	20		6549.778	6851.791		1006.751	1152.429		145.1065	193.0733
	30		4881.814	5183.828		821.0075	966.6846		138.1418	186.1086
	40		4132.875	4434.888		727.2533	872.9303		139.1833	187.1501
	50		3543.585	3845.598		66.7075	811.3845		132.2639	180.2308
	60		3076.361	3378.374		645.9385	791.6156		125.5808	173.5477
	70		2807.198	3109.212		636.8341	782.5111		126.5063	17404731
	80		2607.236	2909.249		646.4644	792.1414		131.1237	179.0905
	90		2476.781	2778.794		620.7997	766.4768		124.079	172.0464
	100		2372.72	2674.733		617.7728	763.4499		117.4237	165.3906
292	10	295.9326	11306.91	11602.84	142.744	1221.486	1364.23	47.00106	92.36795	139.369
	20		6596.461	6892.393		1037.462	1180.206		95.48578	142.4868
	30		4969.981	5264.981		886.5372	1029.281		92.14573	139.1468
	40		4145.573	4441.505		774.6538	917.3978		86.71645	133.7175
	50		3592.505	3888.437		699.1268	841.8708		89.70063	136.7017
	60		3162.454	3458.386		658.6013	801.3452		93.44842	140.4495
	70		2876.023	3171.955		635.0841	777.828		85.88815	132.8892
	80		2630.957	2926.89		626.0259	768.7699		87.99552	134.9966
	90		2502.195	2798.128		605.8815	748.6255		86.50342	133.5045
	100		2338.346	2634.279		585.2866	728.0305		88.71257	135.7136

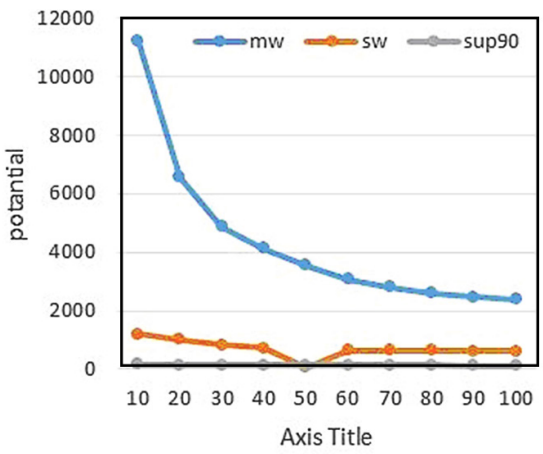

Fig. 1. potential energy of sup-90-amber method-315 kelvin.

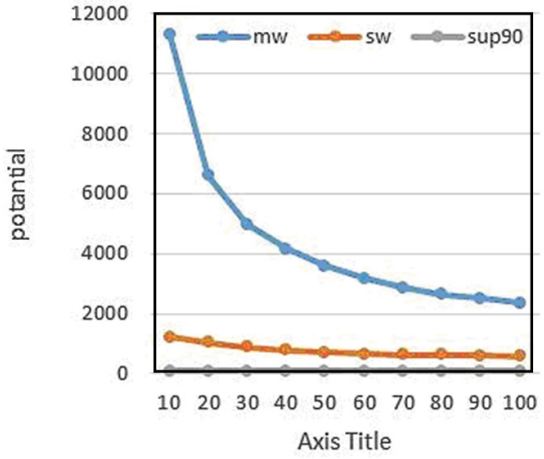

Fig. 2. potential energy of sup-90-amber method-310 kelvin.

Table 2. Bio force field of sup-90

T(K)	Time step Ns	mw-sup90-DOTA-Hmn14(Kcal/mol)			sw-sup90-DOTA-Hmn14(Kcal/mol)			sup90-DOTA-Hmn14(Kcal/mol)		
		Kinetic energy	Potential energy	Total energy	Kinetic energy	Potential energy	Total energy	Kinetic energy	Potential energy	Total energy
315	10	236.6149	5200.743	5437.358	153.9875	576.1253	730.1128	50.7032	131.4211	182.1243
	20		3407.702	3644.317		525.7985	679.786		126.44	177.1432
	30		2620.194	2856.809		501.3898	655.3772		122.4437	173.1469
	40		2190.681	2427.296		455.3535	609.341		130.5071	181.2103
	50		1886.865	2123.48		426.2918	580.2793		124.463	175.1662
	60		1675.062	1911.677		419.5972	573.5847		127.8161	178.5192
	70		1587.852	1824.467		413.6519	567.6394		121.0168	171.72
	80		1494.013	1730.628		384.8939	538.8814		125.0728	175.776
310	90	232.8591	1474.486	1711.101	151.5432	368.4984	522.4859	49.89838	120.6005	171.3037
	100		1440.411	1677.026		385.787	539.7745		125.8001	176.5033
	10		5590.293	5823.152		583.7134	735.2566		95.5857	145.4841
	20		3528.038	3760.897		517.2235	668.7668		93.64977	143.5481
	30		2713.846	2946.705		504.8069	656.3502		95.8878	145.7862
	40		2290.172	2523.031		447.3808	598.9241		93.13429	143.0327
	50		1960.75	2193.609		427.3493	578.8925		94.0752	143.9736
	60		1763.611	1996.47		397.5305	549.0737		95.90796	145.8063
298	70	223.8452	1657.928	1890.787	145.677	391.5584	543.1016	47.96683	86.84603	136.7444
	80		1547.412	1780.272		384.6976	536.2408		98.11166	148.01
	90		1495.969	1728.828		374.2544	525.7976		93.61631	143.5147
	100		1470.669	1703.528		386.4156	537.9589		86.63778	136.5362
	10		5375.414	5599.259		560.5623	706.2394		95.86876	143.8356
	20		3407.525	3631.37		485.8002	631.4772		95.78199	143.7488
	30		2645.07	2868.915		478.8794	624.5564		99.01215	146.979
	40		2207.36	2431.205		439.7843	585.4614		101.4007	149.3676
292	50	219.3383	1922.547	2146.392	142.744	429.4863	575.1634	47.00106	98.89664	146.8635
	60		1695.532	1919.377		404.9038	550.5809		100.3604	148.3272
	70		1607.579	1831.425		399.8531	545.5302		94.0802	142.047
	80		1521.279	1745.124		395.7118	541.3889		93.30536	141.2722
	90		1468.066	1691.911		377.4242	523.1012		92.88617	140.853
	100		1418.363	1642.208		373.4531	519.1302		95.43455	143.4014
	10		5281.936	5501.275		573.2023	715.9462		95.2067	142.2078
	20		3470.879	3690.217		509.805	652.5489		88.84551	135.8466
	30		2688.342	2907.681		471.527	614.2709		92.45333	139.4544
	40		2221.582	2440.92		419.7306	562.4745		89.21799	136.2191
	50		1905.624	2124.962		398.4022	541.1462		101.2364	148.2375
	60		1707.008	1926.346		392.5698	535.3138		101.6836	148.6847
	70		1586.645	1805.983		383.4124	526.1564		97.72719	144.7282
	80		1482.386	1701.724		371.6894	514.4333		101.8406	148.8417
	90		1440.734	1660.073		340.4852	483.2291		97.54325	144.5443
	100		1414.486	1633.824		361.8596	504.6036		95.78306	142.7841

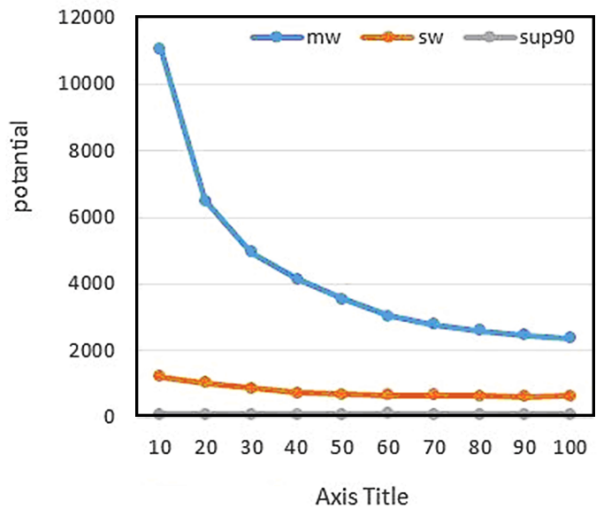

Fig. 3. potential energy of sup-90-amber method-298 kelvin.

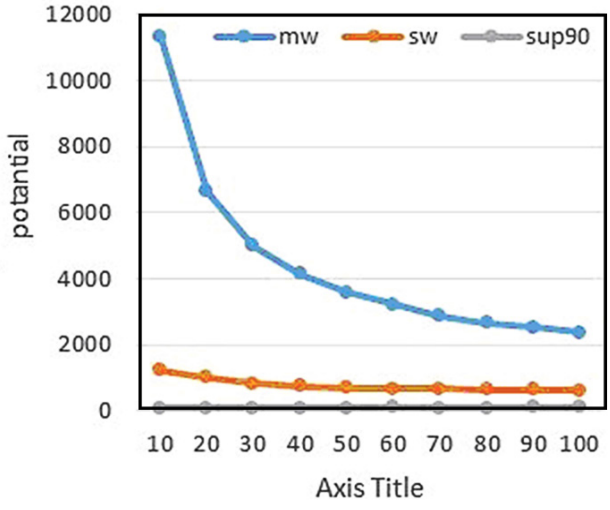

Fig. 4. potential energy of sup-90-amber method-292 kelvin.

Table 3. Mm+ force field of sup-90

T(K)	Time step Ns	mw-sup90-DOTA-Hmn14(Kcal/mol)			sw-sup90-DOTA-Hmn14(Kcal/mol)			sup90-DOTA-Hmn14(Kcal/mol)		
		Kinetic energy	Potential energy	Total energy	Kinetic energy	Potential energy	Total energy	Kinetic energy	Potential energy	Total energy
315	10	319.2423	4001.685	4320.927	153.9875	476.8349	630.8224	50.7032	120.9968	171.7
	20		2920.591	3239.834		461.2152	615.2027		121.8205	172.5237
	30		2429.888	2749.13		429.5299	583.5174		122.243	172.9462
	40		2167.259	2486.501		408.2566	562.244		121.7494	172.4526
	50		1930.89	2250.132		399.5052	553.4927		119.7995	170.5027
	60		1800.401	2119.644		405.5517	559.5392		125.2046	175.9078
	70		1719.389	2038.631		387.9828	541.9703		126.4247	177.1279
	80		1679.842	1999.084		376.6615	530.649		119.2487	169.9519
310	90	314.175	1645.398	1964.64	151.5432	381.855	535.8425	49.89838	121.3022	172.0054
	100		1582.803	1902.045		380.4397	534.4272		114.5615	165.2647
	10		2680.914	2995.089		478.3692	629.9125		124.0741	173.9725
	20		2212.199	2526.374		452.3352	603.8784		125.4202	175.3186
	30		1907.981	2222.156		415.8451	567.3883		127.8544	177.7528
	40		1717.394	2031.569		401.1619	552.7052		128.4171	178.3155
	50		1588.847	1903.022		403.466	555.0092		132.292	182.1903
	60		1533.713	1847.888		391.3759	542.9191		126.6307	176.5291
298	70	302.0134	1465.702	1779.877	145.677	386.8405	538.3837	47.96683	127.314	177.2124
	80		1423.377	1737.552		389.2567	540.8		122.1491	172.0475
	90		1357.85	1672.025		366.2753	517.8186		126.022	175.9203
	100		1304.561	1618.736		374.4256	525.9688		116.4054	166.3037
	10		2667.929	2969.942		469.4612	615.1382		126.0384	174.0053
	20		2195.35	2497.363		434.9642	580.6412		131.5602	179.5271
	30		1904.815	2206.828		408.1015	553.7786		117.5919	165.5587
	40		1704.118	2006.132		394.3995	540.0765		120.6267	168.5936
	50		1571.119	1873.133		369.0641	514.7412		120.8664	168.8332
292	60	295.9326	1470.842	1772.855	142.744	370.9333	516.6104	47.00106	117.2172	165.184
	70		1423.199	1725.212		356.5528	502.2298		115.8696	163.8364
	80		1378.303	1680.317		366.8574	512.5345		117.4475	165.4143
	90		1348.217	1650.231		350.1537	495.8307		114.0635	162.0303
	100		1286.216	1588.23		357.0942	502.7713		122.6844	170.6513
	10		2676.93	2972.862		485.7023	628.4462		12304844	170.4855
	20		2168.294	2464.226		438.1817	580.9256		114.2564	161.2575
	30		1928.981	2224.914		433.2593	576.0033		119.534	166.5351
	40		1751.833	2047.766		380.2508	522.9948		114.0296	161.0307
	50		1608.985	1904.918		390.7845	533.5285		116.1856	163.1867
	60		1515.709	1811.641		365.138	507.882		113.5236	160.5246
	70		1440.437	1736.37		368.0954	510.8394		115.9632	162.9642
	80		1400.487	1696.42		358.6442	501.3881		119.8475	166.8486
	90		1338.921	1634.853		366.1652	508.9091		125.4678	172.4689
	100		1298.536	1594.469		372.8374	515.5814		118.1542	165.1553

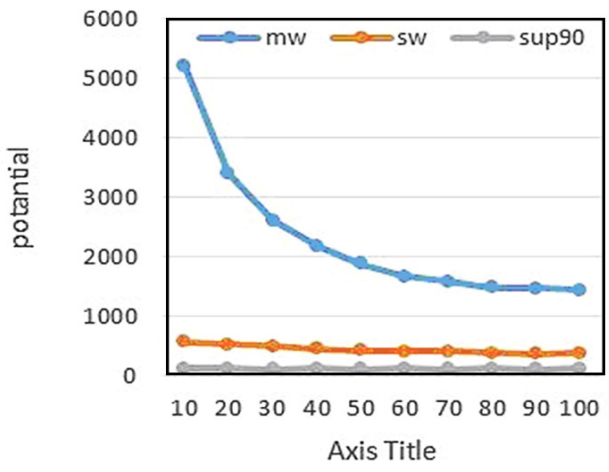

Fig. 5. potential energy of sup-90-bio method-315 kelvin.

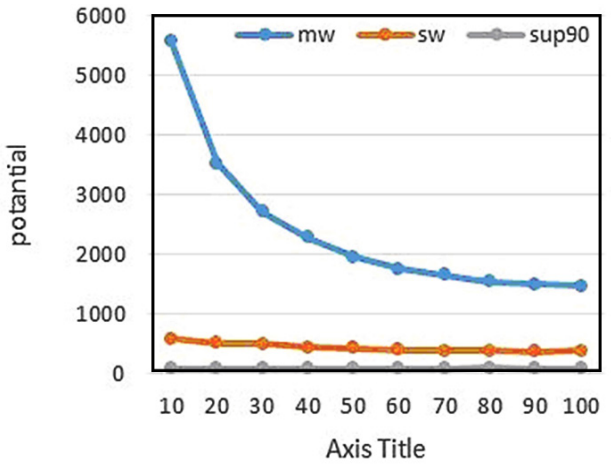

Fig. 6. potential energy of sup-90-bio method-310 kelvin.

Table 4. Opls force field of sup-90

T(K)	Time step Ns	mw-sup90-DOTA-Hmn14(Kcal/mol)			sw-sup90-DOTA-Hmn14(Kcal/mol)			sup90-DOTA-Hmn14(Kcal/mol)		
		Kinetic energy	Potential energy	Total energy	Kinetic energy	Potential energy	Total energy	Kinetic energy	Potential energy	Total energy
315	10	236.6149	11673.58	11910.2	153.9875	1090.333	1244.32	50.7032	90.83673	141.5399
	20		6730.655	6967.27		873.2247	1027.212		82.64115	133.3443
	30		4914.399	5151.014		727.5198	881.5073		86.95129	137.6545
	40		3976.464	4213.079		611.8653	765.8527		90.90554	141.6087
	50		3325.618	3562.233		527.3499	681.3374		91.61191	142.3151
	60		2900.378	3136.993		494.9106	648.898		90.79926	141.5025
	70		2554.069	2790.684		477.4904	631.4779		92.48832	143.1915
	80		2347.031	2583.646		445.1411	599.1286		83.36599	134.0692
	90		2212.07	2448.685		436.1668	590.1542		99.6402	150.3434
	100		2150.932	2387.547		426.5911	580.5786		87.16982	137.873
310	10	232.8591	12260.43	12493.29	151.5432	1073.457	1225	49.89838	96.76836	146.6667
	20		6756.491	6989.35		886.58	1038.123		90.42548	140.3239
	30		4882.521	5115.38		686.7781	838.3213		104.5541	154.4525
	40		3987.404	4220.263		581.2941	732.8373		96.39605	146.2944
	50		3331.15	3564.009		512.1762	663.7195		96.66811	146.5665
	60		2883.55	3116.409		486.4321	637.9754		100.4861	150.3845
	70		2618.153	2851.012		461.8281	613.3713		86.43059	136.329
	80		2407.249	2640.108		441.5641	593.1074		90.68325	140.5816
	90		2278.912	2511.771		417.8375	569.3808		87.52301	137.4214
	100		2179.147	2412.006		407.0963	558.6395		87.17457	137.073
298	10	223.8452	11569.48	11793.32	145.677	1046.905	1192.582	47.96683	95.86756	143.8344
	20		6682.805	6906.65		841.9522	987.6293		97.11809	145.0849
	30		4941.751	5165.597		633.5704	779.2474		88.16172	136.1285
	40		3989.928	4213.773		522.8909	668.5679		88.10602	136.0729
	50		3361.072	3584.917		465.8239	611.5009		90.66873	138.6356
	60		2909.944	3133.789		439.0334	584.7104		92.12326	140.0901
	70		2551.135	2774.98		422.0905	567.7675		92.52257	140.4894
	80		2331.334	2555.179		402.4818	548.1588		89.55149	137.5183
	90		2194.531	2418.376		393.936	539.6131		91.97839	139.9452
	100		2125.701	2349.546		414.4859	560.1629		84.03211	131.9989
292	10	219.3383	12057.6	12276.93	142.744	1031.612	1174.356	47.00106	107.7123	154.7133
	20		6764.794	6984.132		826.9286	969.6726		98.86029	145.8613
	30		4986.652	5205.99		654.9742	797.7181		97.28829	144.2893
	40		3974.55	4193.889		545.5147	688.2587		96.5826	143.5837
	50		3367.86	3587.198		479.9777	622.7217		86.51515	133.5162
	60		2938.873	3158.211		444.2825	587.0264		83.64954	130.6506
	70		2582.384	2801.722		443.2612	586.0052		79.92876	126.9298
	80		2357.444	2576.782		422.8765	565.6205		76.30439	123.3054
	90		2201.509	2420.847		394.5367	537.2806		78.68877	125.6898
	100		2101.179	2320.518		398.1613	540.9053		77.69116	124.6922

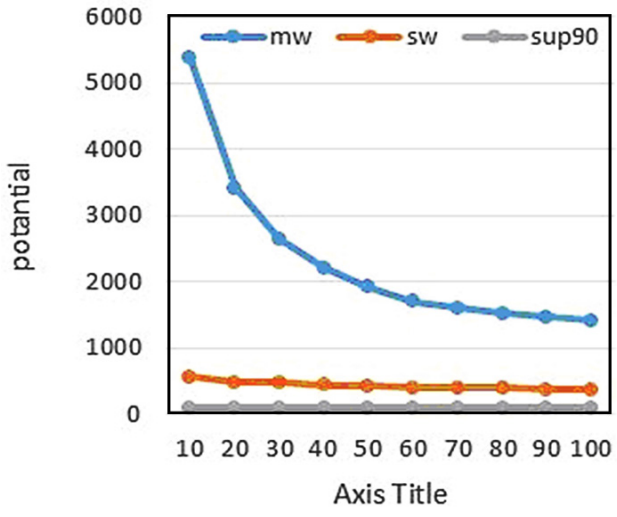

Fig. 7. potential energy of sup-90-bio method-298 kelvin.

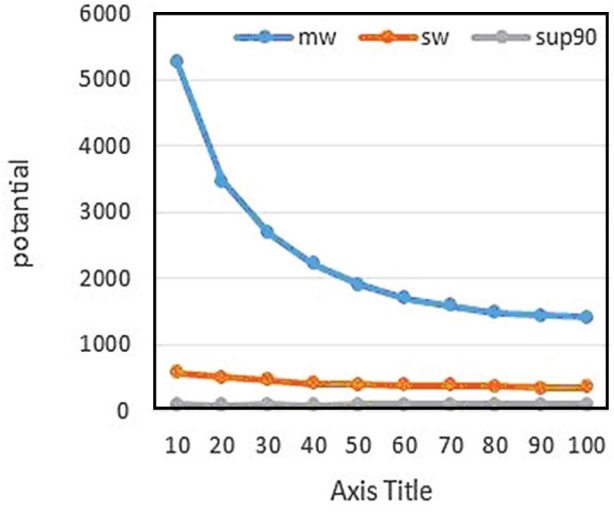

Fig. 8. potential energy of sup-90-bio method-292 kelvin.

Table 5. Semi Empirical method of sup-90

	AM1			CNDO		
	Mw-sup90	Sw-sup90	Sup90	Mw-sup90	Sw-sup90	Sup90
Total Energy	3630702.35	1312068.9101712	-130800.303	4083718.394	1825802.7752002	-55539.74686
Binding energy	4217294.40	1693854.1887432	-5023.48738	4911365.213	2368495.7518763	130960.9268
Isolated atomic energy	-586592.05	-381785.2785720	-125776.8156	-827646.8191	-542692.9766762	-186500.6737
Electronic energy	-14579164.71	-6232175.1590821	-1088963.721	-14882589.61	-6055279.4115323	-1082191.015
Core-core interaction	18209867.06	7544244.0692533	958163.4178	18966308.01	7881082.1867325	1026651.268
Heat of formation	4251925.06	1715347.1337432	4731761.37	4945995.87	2389988.6968763	136031.7318

Table 6. Semi Empirical method of sup-90

	INDO			MINDO3		
	Mw-sup90	Sw-sup90	Sup90	Mw-sup90	Sw-sup90	Sup90
Total Energy	3670623.588	1384918.4529845	60465.03071	3181931.866	1029777.6042889	59332.351
Binding energy	4467838.802	1907573.4138229	239919.6748	3761408.905	1406273.5657789	182101.9661
Isolated atomic energy	-797215.2142	-522654.9608384	-179454.6441	-579477.0386	-376495.961490	-122769.6151
Electronic energy	-15295684.41	-6496163.7337480	-966186.2377	-14860514.01	-6442268.7100817	-885656.9644
Core-core interaction	18966308.01	7881082.1867325	1026651.268	18042445.87	7472046.3143706	944989.3154
Heat of formation	4502469.459	1929066.3588229	244990.4798	3796039.562	1427766.5107789	187172.7711

Table 7. Semi Empirical method of sup-90

	MNDO-d			MNDO		
	Mw-sup90	Sw-sup90	Sup90	Mw-sup90	Sw-sup90	Sup90
Total Energy	2851061.796	-402147.0269812	-22232.81635	2851061.796	-402147.026981	-131183.773225
Binding energy	3437393.787	-20286.9615862	104037.3432	3437393.787	-20286.961586	-4913.613640
Isolated atomic energy	-586331.99	-381860.065395	-126270.1596	-586331.99	-381860.065395	-126270.159585
Electronic energy	-15364207.77	-7949322.966109	-981103.216	-15364207.77	-7949322.966110	-1090054.172834
Core-core interaction	18215269.57	7547175.9391286	958870.3996	18215269.57	7547175.939128	958870.39960
Heat of formation	3472024.444	1205.9834138	109108.1482	3472024.444	1205.9834138	157.1913599

Table 8. Semi Empirical method of sup-90

	PM3			RM1		
	Mw-sup90	Sw-sup90	Sup90	Mw-sup90	Sw-sup90	Sup90
Total Energy	3226865.558	-170125.4832216	59473.5432371	3638531.056	1109940.6104115	69069.4975286
Binding energy	3767021.747	180521.6801004	173234.4247991	4225123.105	1491725.8889835	194846.3131406
Isolated atomic energy	-540156.1887	-350647.1633220	-113760.881562	-586592.050	-381785.2785720	-125776.815612
Electronic energy	-14870198.66	-7668151.016393	-892884.022020	-14568700.91	-6433247.130892	-888843.388438
Core-core interaction	18097064.22	7498025.5331717	952357.5652576	18207231.97	7543187.7413034	957912.8859667
Heat of formation	3801652.404	202014.6251004	178305.2297991	4259753.762	1513218.8339835	199917.1181406

cations. These equations are solved iteratively to the point where the results do not vary significantly between two iterations. It is noteworthy that CNDO does not involve knowledge about chemical bonds but instead uses knowledge about quantum wave functions. CNDO can be used for both closed-shell molecules, where the electrons are fully paired in molecular orbitals and open-shell molecules, which are radicals with unpaired electrons. It is also used in solid state and nanostructures calculations (Abdulsattar, 2009).

CNDO is considered to yield good results for partial atomic charges and molecular dipole moment. Total energy and binding energy are calculated. Eigenvalues for calculating the highest occupied molecular orbital and lowest unoccupied molecular orbital are reported from the closed shell approach. INDO stands

Table 9. Semi Empirical method of sup-90

	ZINDO1			ZINDOS		
	Mw-sup90	Sw-sup90	Sup90	Mw-sup90	Sw-sup90	Sup90
Total Energy	3721544.946	1769894.6956324	68216.8680362	2413603.226	1194457.150907	-148362.269873
Binding energy	4474458.842	2263610.4548459	237934.9561583	3008013.059	1580680.324063	-22372.4225085
Isolated atomic energy	-752913.8961	-493715.7592135	-169718.088122	-594409.830	-386223.173156	-125989.847364
Electronic energy	-15244763.06	-6111187.491101	-958434.400415	-14872759.2	-5951219.776331	-998825.736154
Core-core interaction	18966308.01	7881082.1867325	1026651.268451	17286362.43	7145676.927238	850463.466281
Heat of formation	4509089.499	2285103.3998459	243005.7611583	3042643.716	1602173.269063	-17301.6175085

for Intermediate Neglect of Differential Overlap. It is a semi-empirical quantum chemistry method that is a development of the complete neglect of differential overlap (CNDO/2) method introduced by John Pople. Like CNDO/2 it uses zero-differential overlap for the two-electron integrals but not for integrals that are over orbitals centered on the same atom (Pople, *et al.*, 1967; Pople & Beveridge, 1970). The method is now rarely used in its original form with some exceptions (Abdulsattar & Al-Bayati, 2007), but it is the basis for several other methods, such as MINDO, ZINDO, and SINDO. ZINDO is a semi-empirical quantum chemistry method used in computational chemistry. It is a development of the INDO method. It stands for Zerner's Intermediate Neglect of Differential Overlap, as it was developed by Michael Zerner and his coworkers in the 1970s (Ridley & Zerner, 1973; Zerner, 1991). Unlike INDO, which was really restricted to organic molecules and those containing the atoms B to F, ZINDO covers a wide range of the periodic table, even including the rare-earth elements. There are two distinct versions of the method:

ZINDO/1 used for calculating ground-state properties such as bond lengths and bond angles. It refers to a SCF (RHF or ROHF) calculation with the INDO/1 level as suggested by Pople, which provides the reference state MO coefficients. Ground-state dipole moments and ionization potentials are in general very accurate. Geometry optimizations are erratic, what prompted Zerner's group to improve the performance of the code in the late 1990s (Da Motta Neto & Zerner, 2001). ZINDO/S (sometimes just called INDO/S) – use the INDO/1 molecular orbitals for calculating excited states and hence electronic spectra. It consists of a CI calculation including only the reference state plus a small set of single-electron excitations within a selected active space, typically five HOMOs and five LUMOs. MINDO or Modified Intermediate Neglect of Differential Overlap is a semi-empirical method for the quantum calculation of molecular electronic structure in computational chemistry. It is based on the Intermediate Neglect of Differential Overlap (INDO) method of John Pople. It was developed by the group of Michael Dewar. The method should actually be referred to as MINDO/3. It was later replaced by the MNDO method, which in turn was replaced by the PM3 and AM1 methods (Bingham, *et al.*, 1975). RM1 is a reparameterization of AM1 for H, C, N, O, P, S, F, Cl, Br, and I (Rocha, *et al.*, 2006).

RESULT AND DISCUSSION

One of the methods in the Hyperchampel program is the Immersion Method. In this method, we examined 6 forces, which we summarize below, in summary, of the following six forces:

- total energy:

The total energy is a sum of the rest energy and the Newtonian kinetic energy.

Which is obtained from the following formula:

$$E \approx m_0 c^2 + \frac{1}{2} m_0 v^2$$

- binding energy:

Binding energy is the energy required to disassemble a whole system into separate parts. A bound system typically has a lower potential energy than the sum of its constituent parts; this is what keeps the system together.

- isolated atomic energy:

Isolated atomic energy is the energy required to form the isolated atom from its valence electrons.

$$E_{isol}(A) = E_{neutralatom}(A) - E_{nucleus}(A) - E_{valenceelectrons}(A)$$

- electronic energy:
Electronics is the science of controlling electrical energy electrically, in which the electrons have a fundamental role.
- core-core interaction:
This energy proves to vary as a function of the valence environment.
- heat of formation:

The heat of formation is defined as the amount of heat absorbed or evolved when one mole of a compound is formed from its constituent elements, each substance being in its normal physical state.

According to the following tables (1-4) we find the following results in examining the Monte Carlo method:

In the study of the Amber force field method at 315k (body temperature), in both nanotubes, single wall and multi-wall potential energy are reduced, But in drug without a nanotube, this energy is reduced (until time step 40) and then increases. Potential energy variations in the combination of the drug with multi-walled nanotubes at the time step of 10 to 100 equal -8686.567. However, this potential energy change in combination with single-walled nanotubes is equal to -589.2545. The total energy in the drug combination with the nanotube has decreased. The kinetic energy has increased in the combination of drug with single-wall nanotubes and this increase has almost doubled in the multi-wall nanotube.

CONCLUSIONS

The kinetic energy for each compound is individually a constant. Therefore, total energy, obtained from the sum of potential energy and kinetic energy, is subject to potential energy changes and is therefore reduced. If stability is greater, the potential difference is less. Sustainability and potential energy are the opposite of each other. If potential changes are compared in each of the three combinations, it shows that wherever the potential difference is negative, the energy is further reduced and more stable. The relation between potential and stability is set out in the table below.

REFERENCES

Forner, A., Llovet, J.M., Bruix, J., (2012). Hepatocellular carcinoma. The Lancet., 379 (9822): 1245–1255.

Kumar, V., Fausto, N., Abbas, A., eds. (2015). Robbins & Cotran Pathologic Basis of Disease (9th Ed.). Saunders.

DeVita, V.T., Lawrence, T.S., Rosenberg, S.A., Weinberg, R.A., DePinho, R.A., (2008). DeVita, Hellman, and Rosenberg's cancer: principles & practice of oncology. Lippincott Williams & Wilkins. Retrieved 9 June 2011.

Kheyfits, A., (2010). Yttrium-90 Radioembolization. Radiology Today. Retrieved 2012.

NNDC contributors (2008). Sonzogni, Alejandro A., (Database Manager), ed. Chart of Nuclides. Upton, New York: National Nuclear Data Center, Brookhaven National Laboratory.

CRC contributors (2007–2008). Yttrium. In Lide, David R. CRC Handbook of Chemistry and Physics. 4. New York: CRC Press.

Audi, G., Bersillon, O., Blachot, J., Wapstra, A.H., (2003). The NUBASE Evaluation of Nuclear and Decay Properties". Nuclear Physics A. Atomic Mass Data Center. 729: 3–128.

Y-90 Handling Precautions. Retrieved 2015-07-15.

Chu, S.Y.F., Ekstrom, L.P., Firestone, R.B., (1999). Table of Isotopes decay data. The Lund/LBNL Nuclear Data Search. Retrieved 2012.

Rault, E., Vandenberghe, S., Staelens, S., Lemahieu, I., (2009). Optimization of Yttrium-90 Bremsstrahlung Imaging with Monte Carlo Simulations. 4th European Conference of the International Federation for Medical and Biological Engineering.

Strontium, Radiation Protection, US EPA. EPA. (April 2012).

PNNL: Isotope Sciences Program - Yttrium-90 Production. PNNL. (February 2012).

Kallini, J.R., Gabr, A., Salem, R., Lewandowski, R.J., (2016). Transarterial Radioembolization with Yttrium-90 for the Treatment of Hepatocellular Carcinoma. Adv Ther. 33 (5): 699-714.

Salem, R., Gordon, A.C., Mouli, S., Hickey, R., Kallini, J., (2016). Y90 Radioembolization Significantly Prolongs Time to Progression Compared

With Chemoembolization in Patients With Hepatocellular Carcinoma. Gastroenterology, 151: 1155–1163.

Salem, R., Gilbertsen, M., Butt, Z., Memon, K., Vouche, M., Hickey, R., Baker, T., Abecassis, M.M., Atassi, R., Riaz, A., Cella, D., Burns, J.L., Ganger, D., Benson, A.B., 3rd Mulcahy, M.F., Kulik, L., Lewandowski, R., (2013). Increased quality of life among hepatocellular carcinoma patients treated with radioembolization, compared with chemoembolization. Clin Gastroenterol Hepatol. 11(10): 1358–1365.

Moghaddam, N.A., Ahmadi, S., Rasoolzadeh, R., (2016). Amino acid binding to nanotube: Simulation of membrane protein channels by computational methods. Biosci. Biotech. Res. Comm., 9 (3): 495-502.

Besharati vineh, M., Rasoolzadeh, R., (2014). Monte Carlo Investigation of Breast Cancer protein and Effects of Tamoxifen and Gleevec. J. Nano Chemical Agriculture, 1 (3): 100-105.

Pople, J. and Beveridge, D., (1970). Approximate Molecular Orbital Theory, McGraw-Hill.

Pople, J.A., Santry D.P. and Segal, G.A., (1965). Approximate Self-Consistent Molecular Orbital Theory. I. Invariant Procedures. J. Chem. Phys., 43: S129-S135.

Pople, J.A. and Segal, G.A., (1965). Approximate Self-Consistent Molecular Orbital Theory. II. Calculations with Complete Neglect of Differential Overlap. J. Chem. Phys., 43, S136-S151.

Pople, J.A. and Segal, G.A., (1966). Approximate Self-consistent Molecular Orbital Theory. III. CNDO results for AB2 and AB3 Systems. J. Chem. Phys., 44, 3289-3296.

Santry, D.P. and Segal, G.A., (1967). Approximate Self-Consistent Molecular Orbital Theory. IV. Calculations on Molecules Including the Elements Sodium through Chlorine. J. Chem. Phys., 47: 158-174.

Abdulsattar, M.A., (2009). Size effects of semiempirical large unit cell method in comparison with nanoclusters properties of diamond-structured covalent semiconductors. Physica E, 41: 1679-1688.

Pople, J., Beveridge, D.L. and Dobosh, P.A., (1967). Approximate self-consistent molecular-orbital theory. V. Intermediate neglect of differential overlap. J. Chem. Phys., 47, 2026-2033.

Pople, J.A. and Beveridge, D., (1970). Approximate Molecular Orbital Theory. McGraw-Hill.

Abdulsattar, M.A. and Al-Bayati, Kh.H., (2007). Corrections and parameterization of semiempirical large unit cell method for covalent semiconductors. Phys. Rev. B, 75: 245201-9.

Ridley, J. and Zerner, M., (1973). An intermediate neglect of differential overlap technique for spectroscopy: Pyrrole and the azines. Theor. Chim. Acta, 32: 111–134.

Zerner, M., (1991). Reviews in Computational Chemistry, Volume 2. Semiempirical Molecular Orbital Methods. Lipkowitz, K.B. and Boyd, D.B. Eds., VCH, New York, 313-365.

Da Motta Neto, J.D. and Zerner, M.C., (2001). New parametrization scheme for the resonance integrals (Hμν) within the INDO/1 approximation. Main group elements. Int. J. Quantum Chem., 81: 187–201.

Bingham, Richard C., Dewar, Michael J.S., Lo, Donald H., (1975). Ground states of molecules. XXV. MINDO/3. Improved version of the MINDO semiempirical SCF-MO method. J. Am. Chem. Soc., 97 (6): 1285-1293.

Rocha, Gerd B., Freire, Ricardo O., Simas, Alfredo M., Stewart, James J.P., (2006). RM1: A reparameterization of AM1 for H, C, N, O, P, S, F, Cl, Br, and I. J. Comput. Chem., 27 (10): 1101-11.

AUTHOR (S) BIOSKETCHES

Amirhosein Esfarjani, MSc., Faculty of Science, Najafabad Branch, Islamic Azad University, Najafabad, Isfahan, Iran

Reza Rasoolzadeh, PhD, Faculty of Science, Najafabad Branch, Islamic Azad University, Najafabad, Isfahan, Iran, *Email: reza.rasoolzadeh@yahoo.com*

Rezvan Mohammadi, MSc., Faculty of Science, Najafabad Branch, Islamic Azad University, Najafabad, Isfahan, Iran